

*Letter to the Editor***HI and OH absorption at  $z = 0.89$** Jayaram N. Chengalur<sup>1</sup>, A.G. de Bruyn<sup>2,3</sup>, and D. Narasimha<sup>4</sup><sup>1</sup> NCRA-TIFR, PO Bag 3, Ganeshkhind, Pune 411007, India<sup>2</sup> Netherlands Foundation for Research in Astronomy, P.O. Box 2, 7990 AA, Dwingeloo, The Netherlands<sup>3</sup> Kapteyn Astronomical Institute, P.O. Box 800, 9700 AA, Groningen, The Netherlands<sup>4</sup> Tata Institute of Fundamental Research, Homi Bhabha Road, Mumbai 400 005, India

Received 19 November 1998 / Accepted 11 January 1999

**Abstract.** We report on WSRT observations of HI and OH absorption at a redshift of  $z = 0.885$  towards the radio lens PKS 1830–21. The mm wave transitions of several molecular species have already been observed in absorption towards PKS 1830–21 at this redshift. At mm wavelengths the source structure is dominated by two extremely compact components, the northeast (NE) and southwest (SW) components. At lower frequencies the continuum emission is much more extended and there is also a broad Einstein ring connecting the NE and SW components. This larger extent of the continuum means that the HI and OH spectra sample a much larger region of the absorber than the mm wave spectra.

The HI spectrum that we obtain is asymmetric, with a peak at  $-147$  km/s with respect to the main molecular line redshift of  $z = 0.88582$ . Weak mm wave molecular absorption has also been detected towards the NE component at this same velocity. The HI absorption, however, covers a total velocity width of 300 km/sec, including velocities well to the red of the deep molecular features, and is fully resolved suggesting that it is spatially widespread. In OH we detect both the 1667 and the 1665 MHz transitions, and the velocity-integrated ratio of their optical depths is consistent with what is expected in thermal equilibrium. The OH spectrum has a velocity width comparable to that of the HI spectrum, suggesting that it too is widespread in the absorber. The lack of a prominent HI peak in the spectrum at the velocity corresponding to the SW component, suggests that the galaxy responsible for the absorption at  $z = 0.885$  has a central molecular disk many kpc in size, and that HI may be deficient in this central region.

Our observations are sensitive to the large scale kinematics of the absorber, and to first order the implied dynamical mass is consistent with the lens models of Nair et al. (1993). Higher spatial resolution is however critical in order to better constrain the lensing models.

**Key words:** cosmology: observations – galaxies: abundances – radio lines: ISM – ISM: abundances

**1. Introduction**

Neutral gas at high redshifts is most easily observed through the Lyman- $\alpha$  transition of the hydrogen atom, which at current technology can be detected in absorption against the UV continuum of QSOs even at column densities as low as  $10^{13}$  atoms/cm<sup>-2</sup>. The bulk (by mass) of the neutral gas however is found in the few very high column density systems (Rao & Briggs, 1993), where one could in principle expect a non trivial molecular fraction. However, quantitative predictions of the molecular fraction are difficult to make since the conversion of gas from atomic to molecular form depends on a variety of environmental factors like the UV background, the metallicity and the dust content, all of which are poorly constrained at high redshift. On the observational front, despite searching a large sample, mm molecular lines have been detected in absorption at high redshifts only from four sources (of which two are gravitational lenses and two appear to arise from gas associated with the AGN itself) (Wiklind & Combes 1998). Here we discuss the case of PKS 1830–21, which is the brightest known radio lens.

PKS 1830–21 was identified as a candidate gravitational lens on the basis of its peculiar radio spectrum and morphology (Rao & Subramanyan 1988, Subramanyan et al. 1990; Jauncey et al. 1991). The radio structure (see Fig. 3) consists of two compact flat spectrum components separated by  $\sim 1''$  (henceforth called the northeast (NE) and southwest (SW) components respectively), joined by a steep spectrum ring. At a frequency of 1.7 GHz roughly one third of the observed flux comes from the ring and each of two compact components. At the redshifted frequencies of HI (753 MHz) and OH (884 MHz) the ring is expected to be even more dominant. The lack of simultaneous, in view of the strong variability, multifrequency flux density observations of sufficient angular resolution makes a more accurate assessment of the ring flux and the relative component fluxes at these low frequencies not possible at present.

For long, no optical counter part has been found for 1830-21 (Djorgovski et al. 1992), largely because of confusion arising from its low galactic latitude, although there is now some evidence for one (Courbin et. al. 1998). Two independent gravi-

**Table 1.** HI observations

Date	Bandwidth MHz (km/s)	Channel Separation (km/s)
03/Nov/96	2.5 (996)	31
15/Nov/96	5.0 (1992)	31
08/Jan/97	2.5 (996)	1

**Table 2.** OH observations

Date	Bandwidth MHz (km/s) <sup>a</sup>	Channel Separation (km/s) <sup>a</sup>
17/Nov/96	5.0 (1696)	26.5
15/Dec/96	5.0 (1696)	26.5

<sup>a</sup> The velocity scale is for the 1667 MHz transition.

tational lensing models have been proposed for PKS 1830–21, (Nair et al. 1993, Kochanek & Narayan 1992). At the time that these models were made no redshift was available either for the source or the lens.

The redshift of the lens is now known to be 0.89 from molecular line observations (Wiklind & Combes 1996). The absorption spectra against the NE and the SW image are very different (Frye et al. 1996, Wiklind & Combes 1998), ruling out the possibility that the molecules at 0.89 are associated with the background quasar itself. The bulk of the molecular absorption occurs against the SW component, although much weaker absorption is also seen in some molecules against the NE component. The velocity separation between the absorption seen against the NE image and the SW image is 147 km/s. In addition to the molecules seen at  $z = 0.88582$ , HI absorption has also been seen towards PKS 1830–21, but at a lower redshift of 0.19 (Lovell et al. 1996). The velocity width of this HI line is  $\sim 30$  km/s and it has been interpreted as arising due to absorption in a dense spiral arm of a low redshift spiral galaxy. No molecular absorption has been detected from this lower redshift system (Wiklind & Combes 1998).

In what follows we report on WSRT observations of the HI and OH absorption arising from the system at  $z = 0.89$ . At mm wavelengths only the extremely compact, flat spectrum components of the background source have sizeable flux. Consequently the spectra sample a region of order only a few tens of parsecs across. At the HI and OH frequencies however, the background source is considerably more extended. These lines are thus more suited to probe the large scale kinematics of the absorbing system as well as to determine the averaged physical properties on a kpc scale.

## 2. Observations and data reduction

The observations were done with the broad band UHF receivers installed at the WSRT as part of the on going WSRT upgrade. The HI observations are summarized in Table 1 and the OH observations in Table 2

The OH observations were made using the standard interferometric mode and the data were reduced using NEWSTAR, the WSRT data reduction package. 1830–21 is spatially unresolved at the WSRT baselines. The data from the two observing runs were added together (after applying the appropriate heliocentric Doppler correction) and is shown in Fig. 2. In addition, a lower resolution but larger total bandwidth spectrum was also obtained. This spectrum (which is not included here) is substantially the same as that shown in Fig. 2. No broader absorption features were detected.

The high resolution HI spectrum, Fig. 1c was obtained using the WSRT as a compound interferometer (CI), where the telescope was divided into two phased arrays and the output of these phased arrays was fed into the correlator. This mode achieves high spectral resolution at the expense of losing spatial information. However since PKS 1830–21 is not resolved at the WSRT, there is no loss of spatial information in the CI mode. The CI data was reduced using the WASP package (Chengalur 1996). The spectrum agrees well with that of Carilli et al. (1997), apart from the region near  $v \sim 0$ , where their spectrum is badly affected by interference. The line is fully resolved and reaches a peak optical depth of 5.5%.

The lower resolution HI spectra Fig. 1a and b were obtained in the standard interferometric mode and reduced using NEWSTAR. The observation on 15 November 1996 used a much larger bandwidth, however again no new broad absorption feature was detected. As in the case for OH (but this time with better sensitivity and a longer time baseline), there is no measurable difference between the spectra obtained over a period of  $\sim 2$  months. The flux densities are calibrated via reference to 3C48 for which we adopt a flux of 25.5 Jy at 753 MHz and 22.7 Jy at 884 MHz which are on the Baars et al. (1977) scale.

## 3. Discussion

With peak optical depths of only 0.007 and 0.005 in the two OH absorption lines the profile shape is not so well defined as that of the HI line. However, it is clear that the OH spectrum and the HI spectrum have similar overall velocity widths. Since the separation of the two OH lines is 350 km/sec we conclude that they do not overlap, consistent with the height of the continuum inbetween the two absorption features.

The 1667 MHz transition has an integrated optical depth that is larger than that of the 1665 MHz transition. Within the measurement errors the ratio of the optical depth is consistent with the 9:5 ratio expected in thermal equilibrium. There is evidence that at zero velocity the 1665 MHz line is deeper than the 1667 MHz line, suggesting variations in opacity of the 1665/1667 transitions. This could be related to the much larger molecular line optical depth at zero velocity than at -147 km/sec. We hope to address this issue with future more sensitive observations of the OH lines.

The optical depth ( $\sim 10^{-2}$ ), the velocity width, the overall optical depth ratio, and the ratio of the OH column density to the excitation temperature ( $N_{\text{OH}}/T_{\text{ex}} \sim 4 \times 10^{14}$ ) are all within the range of OH absorption seen towards the centers of low

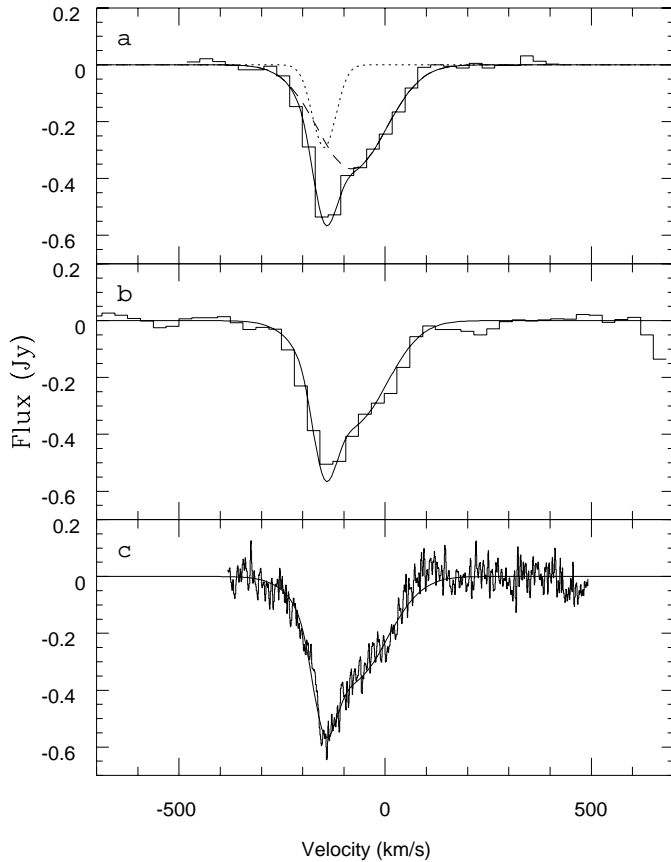


**Fig. 1a–c.** HI spectrum at  $z = 0.89$  towards PKS 1830–21. **a** The velocity resolution is 31 km/s. The velocity scale here and throughout the paper is with respect to the molecular absorption towards the SW image at  $z_{\text{hel}} = 0.88582$ . The solid line is a two gaussian fit to the spectrum, the component gaussians are shown by dotted and dashed lines respectively. The position and FWHM of the narrow gaussian are  $-148$  km/s and 40 km/s respectively. The position and FWHM of the broader gaussian is  $-80$  km/s and 120 km/s respectively. **b** The HI spectrum again at a resolution of 31 km/s, but with a total bandwidth of  $\sim 2000$  km/s. No broad absorption is seen, nor are any narrow absorption components seen at large velocities. The overlaid solid line is the fit to spectrum in part **a**. **c** The CI spectrum with a resolution of  $\sim 1$  km/s. Once again the superimposed solid line is not a separate fit, but the same fit as in panel **a**. No new narrow absorption features are seen. The continuum flux of PKS 1830–211 at the observed frequency is about 10.5 Jy

redshift galaxies (Schmeltz et al. 1986). Under the assumption that the absorption arises from a rotating galaxy disk, the large OH velocity width implies that the covering factor of the OH absorbing gas is  $\sim 1$ . In the Nair et. al. model, the distances of the SW and NE images from the lens center are 1.8 kpc and 3.8 kpc respectively (for  $H_0 = 75$  km/s/Mpc and  $q_0 = 0.5$ ), and hence OH would have to be widespread in the central 5–6 kpc of the galaxy.

The HI spectrum is highly asymmetric, with a peak at  $-148$  km/s, the same velocity where weak molecular absorption is seen against the NE core. The HI peak is then presumably gas seen in absorption against the very compact NE compo-

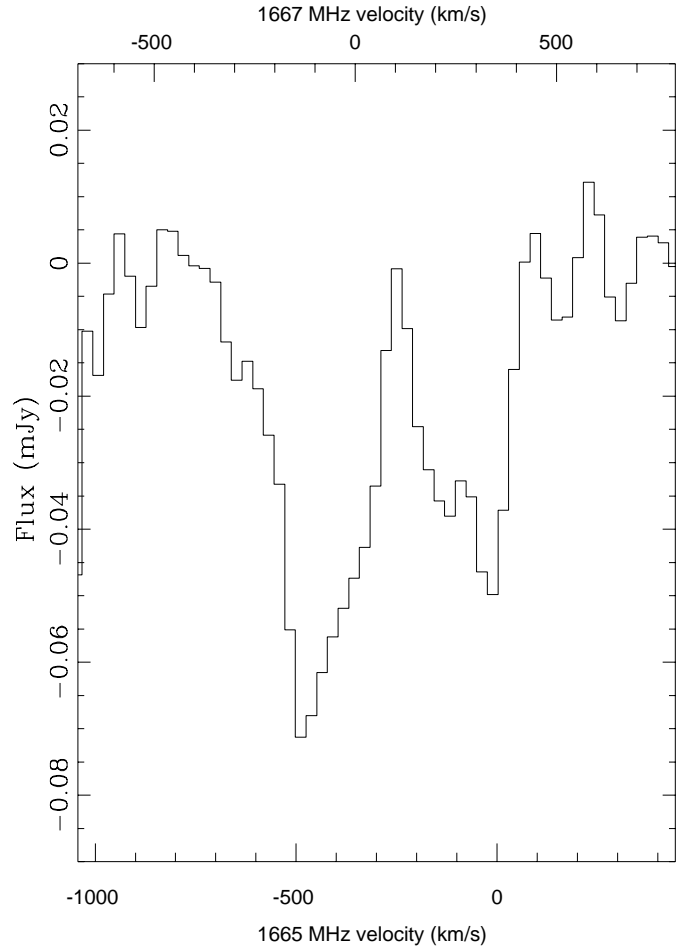


**Fig. 2.** OH spectrum at  $z = 0.89$  towards PKS 1830–21. The lower axis shows the velocity scale (with respect to  $z = 0.88582$ ) for the 1667 MHz transition, while the velocity scale for the 1665 MHz transition is shown in the upper axis. The velocity resolution is  $\sim 27$  km/s. The continuum flux at the observed frequency of 884 MHz is about 10.1 Jy

nent. If one assumes that this component has  $\sim 1/3$  of the total flux then for the gas lying in front of the NE component  $N_{\text{H}}/T_{\text{spin}} \sim 3 \cdot 10^{19}$ , compatible with galactic numbers of  $N_{\text{H}} \sim 3 \cdot 10^{21}$  cm $^{-2}$ , and  $T_{\text{spin}} \sim 100$  K.

The red wing of the HI absorption profile shows a weak but resolved feature at zero velocity, corresponding to the deep molecular absorption. The contrast in the ratio of HI optical depth at the two velocities, compared to that of the OH molecules, is striking. One possibility is that the gas in front of the SW component is primarily molecular, (i.e. similar to what is seen in many early type spirals). Because the size of the radio source at 753 MHz is estimated to be at least 200 milliarcseconds (cf Patnaik & Porcas, 1995) corresponding about 1.5 kpc, several orders of magnitude larger than at mm wavelengths, this lack of HI must indicate a genuine lack of HI in a substantial part of the inner galaxy. This, in conjunction with the OH spectrum, then suggests that the  $z = 0.89$  system is an early type spiral with a large central molecular disk, at least 5–6 kpc in size. The

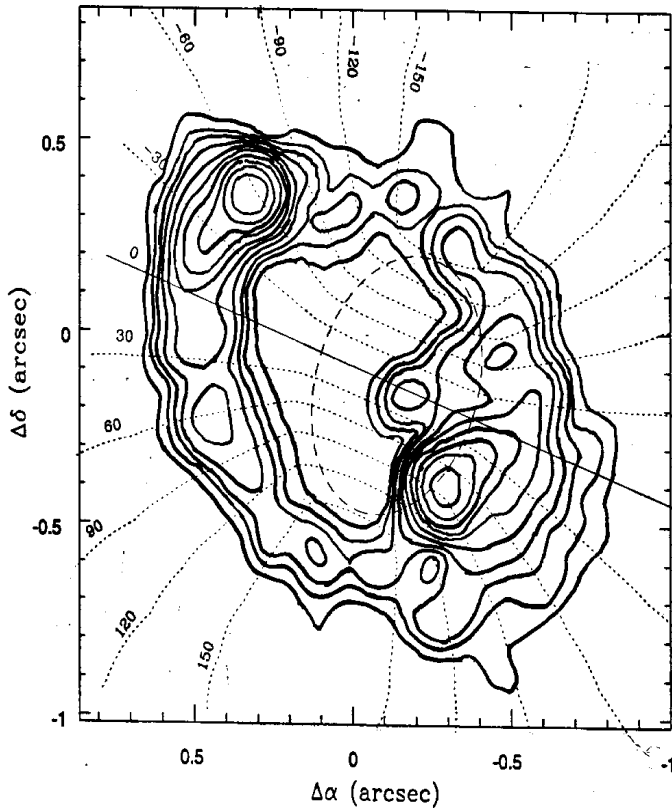


**Fig. 3.** Schematic showing PKS 1830–21 superposed on a typical galactic velocity field. The galaxy inclination and position angle are close to that of the best fit model in Nair et al. 1993. The radio contours are from the 6cm MERLIN image of Patnaik et al. 1994

broad component in the HI spectrum is presumably the result of HI seen in absorption primarily against the steep spectrum ring.

Since at low frequencies the ring has no gaps and the center of the lensing galaxy must lie inside the ring, then without recourse to any specific lensing model it follows that the ring must cut across both the receding and approaching sides of the major axis (Fig. 3). For reasonable rotation curves the ring will cut across the major axis well beyond the rising part of the rotation curve. In principle then, the velocity width of the HI spectrum ( $\sim 260$  km/s) corresponds to twice the rotation velocity of the galaxy (apart from an inclination correction). In practice however since the emission from the ring is weakest at the points where it cuts across the major axis, the rotation velocity could be somewhat underestimated. From the model in Nair et al. (1993) it is straightforward to compute the velocity

that one should see in absorption against the SW and the NE cores. The observed velocities are indeed obtained provided one changes the position angle slightly. The inclination angle in the Nair et al. model is  $\sim 40^\circ$ , however this gives the mass inside the central 4 kpc as  $\sim 4 \times 10^{10} M_\odot$ , which is somewhat low for a source redshift  $\sim 1.5-2$ . As suggested by Wiklind & Combes (1998), the inclination angle may be closer to  $\sim 20^\circ$ , and the true rotation velocity more like  $\sim 300$  km/s, more typical of early type spirals.

In summary then, the OH and HI spectra are consistent with the lens being an early type spiral at a redshift of  $z \sim 0.89$ .

*Acknowledgements.* We are grateful for the extensive support provided by the WSRT staff in scheduling and preparing these observations which were done in the middle of a band filled with strong RFI. The WSRT is operated by the Netherlands Foundation for Research in Astronomy (NFRA) with financial support by the Netherlands Organization for Scientific Research (NWO). This research was supported in part by the European Commission, TMR Programme, Research Network Contract ERBFMRXCT96-0034 'CERES'

## References

- Baars, J.W.M., Genzel, R. Paulini-Toth, I.I.K. & Witzel, A. 1977, *A&A* 61, 99
- Carilli, C. L., Menten, K.M., Reid, M.J., Rupen, M.P. and Claussen, M. astro-ph 9801157
- Chengalur, J. N., NFRA note 453, 1996
- Courbin, F. et al., 1998 to appear in *ApJL*
- Djorgovski, S., et al., 1992 *MNRAS* 257, 240
- Frye B., Welch, W. J., & Broadhurst, T., 1997 *ApJ* 478, L25
- Jauncey, D. L. et al., 1991 *Nature* 352, 132
- Kochanek, C. S. & Narayan R., 1992 *ApJ* 401, 461
- Lovell, J.E.J. et al., 1996 *ApJ*, 472, L5
- Nair S., Narasimha D., & Rao, A. P. 1993 *ApJ* 407, 46
- van Ommen, T. Jones, D. Preston R. & Jauncey, D. 1995, *ApJ* 444, 561
- Patnaik, A. et al. 1994, In: Proceedings of the 1993 Liege Symposium on Gravitational Lensing
- Patnaik, A. & Porcas, R. 1995, In: Kochanek, C.S. and Hewitt, J.N. Proc. IAU Symposium 173, Astrophysical Applications of Gravitational Lensing, Kluwer Academic Publishers
- Rao, A. P. & Subramanian, R., 1988 *MNRAS* 231, 229
- Rao, S. & Briggs, F. 1993, *ApJ* 419, 515
- Schmeltz, J. T., Baan, W. A., Haschick, A. D., & Eder, J. 1986 *AJ* 92, 1291
- Subramanian, R., Narasimha, D., Rao, A. P., & Swarup, G. 1990 *MNRAS* 246, 263
- Wiklind, T. & Combes, F., 1996 *Nature* 379, 139
- Wiklind, T. & Combes, F., 1998 *ApJ* 500, 129